J. Physiol. (1979), **288**, *pp.* 263–284
With 12 text-figures
Printed in Great Britain

VOLTAGE-CLAMP ANALYSIS OF THE POTASSIUM CURRENT THAT PRODUCES A NEGATIVE-GOING ACTION POTENTIAL IN *ASCARIS* MUSCLE

BY LOU BYERLY AND MASAKO O. MASUDA*

From the Department of Physiology, University of California at Los Angeles, Los Angeles, California, 90024, U.S.A.

(*Received 23 May 1978*)

SUMMARY

1. A voltage clamp has been developed for the pharyngeal muscle of the nematode *Ascaris lumbricoides* and has been used to analyse the potassium current that produces a negative-going, regenerative action potential in this muscle.

2. Depolarizing voltage steps elicit a sustained inward current; returning the membrane voltage to the resting level evokes a strong, transient, outward current. This outward current reverses direction at the same voltage as that reached by the negative-going spike and is identified as the negative spike current.

3. The negative spike current decays with a time constant of 30 msec at voltages more negative than -30 mV. This inactivation of the negative spike conductance is removed by holding the membrane at potentials more positive than -15 mV. The time constant for removal of inactivation decreases from more than 300 msec at -15 mV to about 30 msec at $+10$ mV.

4. When inactivation has been removed, the negative spike conductance is turned on by stepping to potentials more negative than -15 mV.

5. Although the reversal potential for this current depends strongly on $[K^+]_o$ (42 mV/decade), the potential at which the conductance is turned on is independent of $[K^+]_o$.

6. External Na^+ seems to facilitate the negative spike current. Reduction of $[Na^+]_o$ reduces its conductance and shifts the reversal potential to more positive values.

7. External Rb^+ and Cs^+ show voltage-dependent blocking of this current.

8. This K current is different from all the K currents which have been studied previously; however, it is analogous to the classical Na current of nerve and muscle, except for an inversion of the voltage dependencies.

INTRODUCTION

The pharyngeal muscle of the parasitic nematode *Ascaris lumbricoides* acts as a pump to force food into the intestine of the animal. It is formed from about thirty cells; during development the boundaries between these cells are lost (Goldschmidt, 1904), and it becomes functionally just one tube-shaped cell (Del Castillo & Morales,

* On leave from Federal University of Rio de Janeiro, Rio de Janeiro, Brazil.

1967*a*), nearly 1 cm long and 1 mm in diameter. When the muscle is relaxed, the triradiate lumen is closed. The contractile fibres are radially oriented (Mapes, 1965; Reger, 1966); depolarization of the cell causes these fibres to shorten, which forces the outer diameter of the cell to expand and the lumen to open, due to the incompressibility of the sarcoplasm. As the lumen opens, fluid from the host's intestine is sucked into the pharynx through a one-way valve near the mouth. When the muscle cell is repolarized, the contractile fibres relax and elastic components that were stretched by the contraction rapidly close the lumen, forcing its contents into the *Ascaris* intestine through a second one-way valve. The hydrostatic pressure inside the animal is greater than outside (Harris & Crofton, 1957), and it is important that the lumen close rapidly in order to overcome this pressure difference.

Del Castillo, De Mello & Morales (1964) first recorded from the pharynx while bathing it with 30% sea water. Under their conditions the resting potential was about -5 mV and negative-going action potentials 110 mV in amplitude could be evoked. In subsequent work (Del Castillo & Morales, 1967*a*) it was found that in a more natural bathing solution, the cell had a resting potential near -35 mV; from this resting potential positive-going, overshooting, often prolonged action potentials could be evoked by applying outward currents. From the plateau of these prolonged action potentials the negative-going action potential could be evoked by applying inward current. They found that the lumen of the pharynx opened relatively slowly after the initiation of a positive-going action potential, remained open during the plateau and closed more quickly during the negative-going action potential. Del Castillo & Morales concluded that the maintained contraction of the prolonged positive-going action potential and its rapid termination by the negative-going spike were features evolved in pharyngeal muscle to improve its efficiency as a pumping device. They also concluded that the negative-going action potential was produced by an increase in the permeability of the membrane to K^+, since the action potential reached a potential that depended on $[K^+]_o$ nearly as expected for a K electrode.

In this paper we report the results of studies done on a section of pharyngeal membrane which was either voltage-clamped or current-clamped. We have concentrated on the properties of the current which produces the negative-going action potential, since this current was the strongest current in the membrane and obviously different from any current which had been previously studied. These studies show that this novel current plays the same role in producing the negative-going action potential in the pharyngeal membrane as does the sodium current in producing the positive-going action potential in squid axon or frog muscle.

METHODS

Ascaris were obtained from Farmer John Packing House, Vernon, California, and maintained in closed jars of artificial perienteric fluid (APF, see Table 1) at 37 °C. Streptomycin sulphate (0·2 g/l.) and K penicillin G (200 u./ml.) were added to the APF solutions used for maintaining the animals. Animals were used within 3 days of the time of collection, since healthy pharyngeal muscles were rarely found at later times. The animal was cut open along one lateral line up to 1–2 mm from the lips, exposing the pharyngeal muscle. The intestine was cut a few millimetres behind the pharynx and used to pull the muscle free from the body wall. The pharynx was then isolated from the rest of the animal by cutting away the body wall, as close to the

front of the pharynx as possible without damaging the muscle. This exposed the entire length of the pharynx, except for the front 1–2 mm, which was still capped by cuticle including the lips. The mean length of the pharynges was 7·7 mm with a standard deviation of 0·6 mm.

Following the observation of Del Castillo & Morales (1967*a*) that action potentials could be recorded in the lumen of the pharynx, a Ag/AgCl wire (insulated except at the tip) was inserted into the lumen of the pharynx. The action potentials recorded from this wire were very similar in shape and 0·5–0·9 times the amplitude of those simultaneously recorded by an intracellular electrode. We interpreted this to mean that the lumenal membrane is not active and that its resistance is of the same size or smaller than the longitudinal resistance along the lumen to the external solution. This suggested to us that current passed from this wire would pass out through the sides of the pharynx, as well as out the ends of the lumen. With a platinized 50 μm silver wire (insulated except for the last 4 mm) in the lumen, we found we could polarize the external membrane by more than 100 mV for prolonged periods of time.

During spontaneous activity the action potential occurs nearly synchronously along the entire length of the pharynx. However, by inserting the pharynx in a tight hole in a rubber diaphragm and passing current from one side to the other of the diaphragm, we found that the electrotonic potential recorded across the external membrane dropped off exponentially with distance away from the diaphragm, falling with a length constant of 1·5–2·0 mm. Since this length constant is small compared to the length of the cell, it was necessary to build our apparatus so that only currents from the membrane near the recording electrode would be measured.

The experimental set-up used for all the studies reported below is shown schematically in Fig. 1. The pharynx is divided into three regions by the two Lucite partitions; the partitions are made like stocks that close down around the pharynx. Vaseline is applied to the Lucite surfaces that close on the pharynx to make a better seal. It is the section of pharynx in the middle compartment that is studied; the mean diameter of the pharynges in this compartment is 0·86 mm with a standard deviation of 0·08 mm. A continual flow of solution bathes this section of membrane, while a separate flow of identical solution bathes the membrane in the two outer compartments. Two glass micro-electrodes (filled with 3 M-KCl) record the potential difference V_m across the external membrane in the middle compartment; the current passing through this membrane I_m is recorded with a virtual-ground, $I \rightarrow V$ converter connected to the bath by a Ag/AgCl plate (positioned just down-stream from the pharynx). Current is injected from the intralumenal electrode as discussed above.

Since there is not a complete seal between the Vaseline and the pharynx, leakage currents under these seals are eliminated by two 'ground-clamp' amplifiers which hold the potentials of the outer baths equal to that of the middle bath. Each ground-clamp amplifier has an offset adjustment so that a correction could be made for the difference in potential measured between the middle and outer baths due to the two different types of recording electrodes used. In practice the adjustment was made by connecting the outputs of the ground-clamp amplifiers to the platinum wires at a time when there was no current flow across the external partitions and $I_m = 0$. After each amplifier was connected to its platinum wire, its offset was adjusted so as to return I_m to zero.

For current-clamp experiments the signal from the $I \rightarrow V$ converter is fed back to the control amplifier (Voltage Clamp System ME3311, Biodyne Electronics Laboratories), which injects the appropriate amount of current through the intralumenal electrode to hold I_m at the value demanded by the command signal. In this way changes in the current flowing through the end segments of the pharynx or out the ends of the lumen will not change I_m. In the voltage-clamp mode V_m is fed back to the control amplifier. When the gain on the control amplifier is turned up to about 10,000, I_m and V_m are clamped effectively and step changes are made to within a few per cent in less than 1 msec.

To test whether I_m comes only from regions of membrane at potential V_m, the potential in various regions of the middle segment of the pharynx was recorded with a second intracellular electrode during voltage-clamp steps and found to always agree with the command signal to within a few millivolts; at the height of the outward K current the largest voltage differences measured by the second electrode was 5 mV. A stronger test of the system is to stimulate action potentials in the front segment of the pharynx, while clamping I_m to zero. If I_m is representative of the current flowing across the membrane where V_m is recorded, then V_m would show no change corresponding to the action potential in the front segment. When I_m was clamped to zero, the

occurrence of action potentials (80 mV amplitude) in the outer segment produced only small hyperpolarization (< 5 mV) in V_m (recorded in the middle chamber). This shows that the set up is basically working as intended, although I_m has a small contribution from regions of membrane affected by the activity in the outer segments. This conclusion is supported by voltage-clamp experiments where the solution bathing the outer segments was altered, but not that bathing the inner segment. This failure to completely isolate electrically the central segment of the pharynx from the outer segments is probably due to the membrane under the Vaseline seal which is presumably still active and contributes current to I_m.

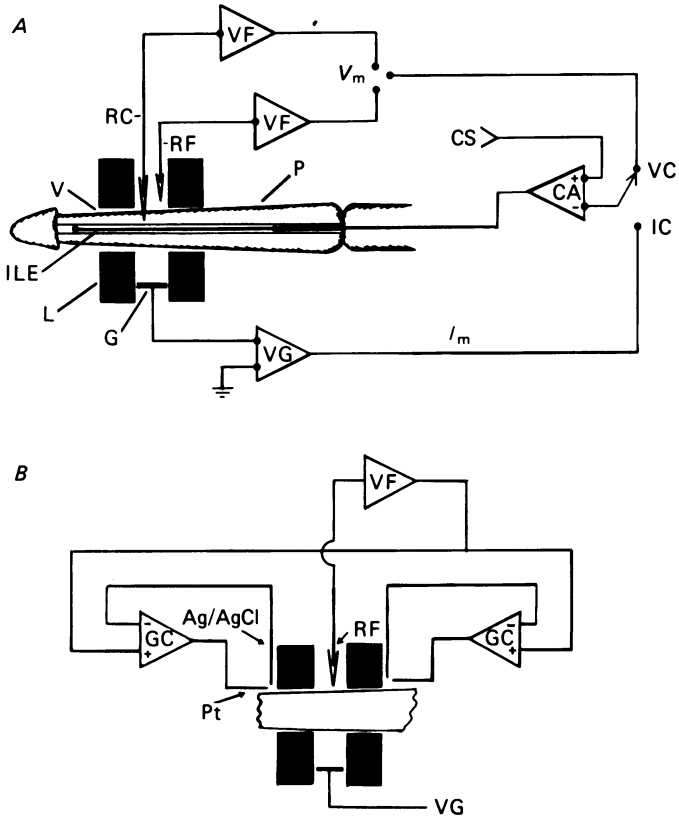

Fig. 1. Experimental set-up. *A*, preparation and schematic diagram of current-clamp and voltage-clamp circuits. The Lucite partitions are each 1·0 mm thick and are separated by 0·8 mm. The holes through the Lucite partitions (in which the pharynx lies) are 1·2 mm in diameter. CA, control amplifier; CS, command signal; G, Ag/AgCl ground electrode; IC, switch position for current-clamp mode; ILE, intralumenal current-passing electrode; L, Lucite partition; P, pharynx; RC, intracellular recording electrode; RF, extracellular reference electrode; V, Vaseline seal between pharynx and Lucite; VC, switch position for voltage-clamp mode; VF, voltage follower amplifier; VG, virtual-ground, current-to-voltage converter. *B*, preparation with schematic diagram of ground-clamp circuits. GC, ground-clamp amplifier, other symbols defined above. Ground-clamp amplifier records outer bath potential through a Ag/AgCl electrode and injects current through a platinum electrode.

Table 1 gives the concentrations of ions in the major solutions used. APF (artificial perienteric fluid) is the standard solution that has been used in previous electrophysiological studies of *Ascaris* (Weisblat, Byerly & Russell, 1976) and is nearly the same as the acetate artificial perienteric fluid used by Del Castillo & Morales (1967*a*). The small amounts (10 mM) of TEA (tetraethylammonium) chloride, 4-AP (4-aminopyridine), RbCl, CsCl and $BaCl_2$ (1 mM) were

simply added to 12 NSF (negative spike fluid), since this did not greatly change the tonicity, All experiments were done between 35 and 36 °C. A somewhat lower temperature than that of the worm's natural habitat was used to reduce spontaneous activity of the pharynx.

TABLE 1. Composition of solutions

Solutions	Ion concentrations (mM)							
	Ca^{2+}	Mg^{2+}	K^+	Na^+	OAc^-	Cl^-	Glucose	Tris*
APF	6	5	24	133	110	78	11	10
O-Ca APF	0	11	24	133	110	78	11	10
X NSF (X = 3–50)	0	11	X	107	110	73 to 78	11	60–X
X Na (Tris) 12 NSF (X = 0–145)	0	11	12	X	110	63 to 78	11	155–X
X Na (glucose) 12 NSF (X = 0–145)	0	11	12	X	$\frac{110X}{145}$	$43+\frac{35X}{145}$	301–2X	10

pH = 7·5 at 36 °C. * Tris = tris (hydroxymethyl) aminomethane.

RESULTS

I. *General electrical properties of the pharyngeal membrane*

Activity under current clamp

Constant-current experiments demonstrate that the pharyngeal membrane can produce both positive-going and negative-going action potentials. When progressively larger outward currents are passed through the external membrane (Fig. 2*A*), the threshold for the positive-going action potential is reached at 10–20 mV above the resting potential; the resting potential is usually −35 to −40 mV. The positive-going action potential overshoots the reference level by 30–50 mV in healthy pharyngeal muscles. The membrane potential then remains positive until it is rapidly returned to negative values by the negative-going action potential, which occurs from 150 msec to several seconds after the positive-going action potential. The negative-going action potential falls to a level determined by $[K^+]_o$; the negative spike reaches about −45 mV in 24 mM-K (Fig. 2*A*) and about −110 mV in 2 mM-K (Fig. 2*C*).

As suggested by the great variation in the duration of the plateau of the positive action potential, the initiation of the negative-going action potential is not coupled to the positive-going action potential, but is independently triggered. The pharynx is innervated by the pharyngeal-sympathetic nervous system (Goldschmidt, 1910), which is embedded in the muscle, lying in invaginations of the external membrane. We are unable to physically separate this nervous system from the pharyngeal muscle, and commonly observe regular i.p.s.p.-like and e.p.s.p.-like events in the membrane potential recorded from our isolated preparation under current-clamp conditions. We assume these actually are post-synaptic potentials resulting from the action of the pharyngeal nervous system. There are two distinct types of p.s.p.s; the reversal potential is about −40 mV for one and about −10 mV for the other. Positive-going p.s.p.s frequently trigger the positive-going action potential when the

membrane potential is at the resting level, and negative-going p.s.p.s can trigger the negative-going spike when the membrane potential is at positive levels. When a constant outward current is passed through the active membrane so as to raise the membrane potential to a level near 0 mV, a series of negative spikes are obtained (Fig. 2*D*), which we assume are triggered by a series of negative-going p.s.p.s.

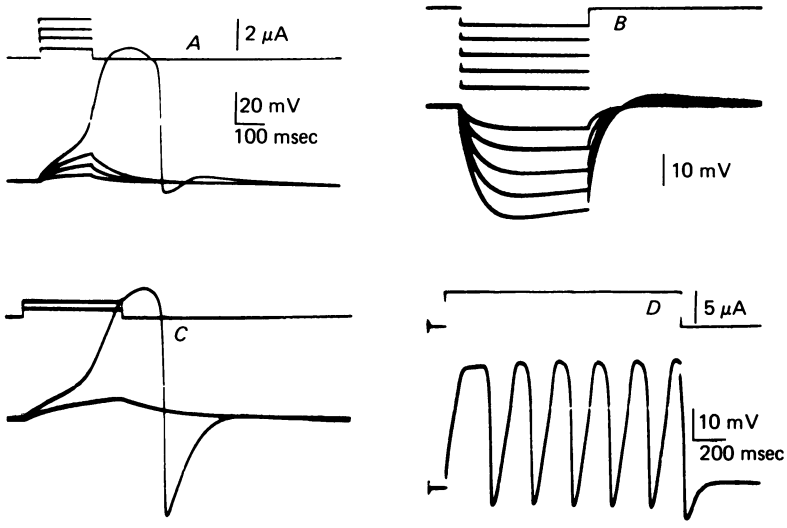

Fig. 2. Intracellular recordings under current-clamp conditions. (Upper traces are I_m; lower traces are V_m.) *A*, outward current pulses; cell in APF. Resting potential is −39 mV; positive action potential reaches +44 mV. *B*, inward current pulses; same cell as in *A*, in APF. *C*, outward current pulses; cell in 2 mM-K^+-APF (K^+ replaced with Na^+). Resting potential is −41 mV; the pharyngeal resting potential does not depend on $[K^+]_o$ when $[K^+]_o$ is less than 30 mM (Del Castillo & Morales, 1967*a*). Positive action potential reaches +47 mV, negative spike reaches −107 mV. *D*, prolonged outward current; cell in APF. Resting potential is −34 mV; most positive potential reached is +3 mV. Calibration is given in *A* and also applies to *B* and *C*, unless otherwise indicated.

Currents under voltage clamp

Voltage-clamp experiments in which the membrane potential is clamped to positive voltage pulses (Fig. 3*A*) immediately reveal the unusual current that produces the negative-going spike; this current is not seen during the voltage pulse, but immediately after it. As the membrane is clamped to more positive levels, the current during the pulse becomes increasingly inward (Fig. 3*C*, circles). Since there is still a net inward current 200 msec after the beginning of the positive pulse, it is clear that this inward current shows little inactivation and that there must be very little delayed rectification in the pharyngeal muscle. Although the nature of this prolonged inward current is of obvious interest due to its importance in maintaining the pharynx depolarized (and contracted) until the negative spike rapidly repolarizes (and relaxes) the pharynx, it will not be discussed in this paper.

Immediately after the termination of the positive pulse a transient outward current flows; the size of this current increases and eventually saturates, as the pulse potential becomes more positive (Fig. 3*C*, squares). Clearly the negative step

at the end of the pulse is turning on a new conductance; otherwise there should be an even larger inward current after the negative step than before. The rate of rise of the measured outward current reflects the decay of the inward capacitance-charging current (discussed below); the new conductance that is turned on by the negative step may open in less than 1 msec. Once this conductance opens, it then inactivates, as demonstrated by the transient nature of this current. Since it will be shown below that this outward current is the current which produces the negative-going action potential, we will refer to it as the negative spike current.

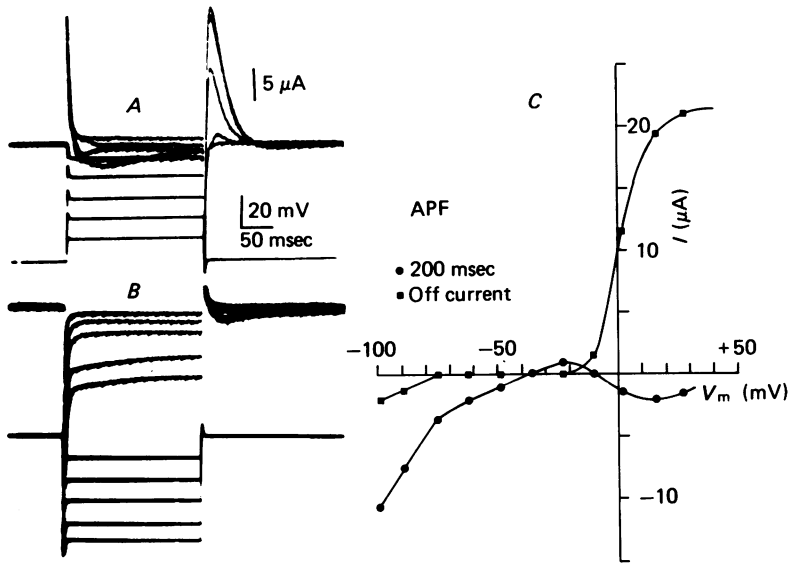

Fig. 3. Single pulse voltage clamps in APF. Upper traces are I_m; lower traces are V_m. All data are from same cell. Holding potential is the resting potential (−37 mV). *A*, positive voltage pulses. *B*, negative voltage pulses. Calibration same as in *A*. *C*, *I–V* plot. The circles show the current measured at the end of the 200 msec pulse (before the termination) as a function of the potential reached by the pulse. The squares show the current 25 msec after the termination of the pulse plotted against the potential of the pulse.

Zero Ca media

Although it seemed most probable that the negative spike current was being turned on directly by the negative step in membrane potential, i.e. that the associated conductance was voltage-dependent, it needed to be demonstrated that this current did not depend on the activity of the pharyngeal nervous system. It was possible that the large currents necessary to repolarize the membrane were directly stimulating a nerve which released a transmitter that turned on the conductance of the negative spike, or that movement of the pharynx triggered the nerves to turn on this current. To rule out the involvement of the nervous system, we bathed the pharynx in 0-Ca APF (see Table 1) to reduce the release of transmitter. In 0-Ca APF e.p.s.p.s were suppressed to an extent that they no longer evoked positive-going action potentials. When a positive-going action potential was evoked by

passing outward current, the membrane potential commonly remained at a positive level for many seconds before the negative spike was triggered, presumably due to the reduced size of the negative p.s.p.s which normally trigger the negative spike. Depolarization of the membrane produced no visible contraction of the pharyngeal membrane in the Ca-free solution. When we voltage-clamped the pharynx in this solution, we found that there were only minor changes in the negative spike current (Fig. 4), confirming the assumption that it was associated with a voltage-dependent conductance. Since the negative spike current persisted in the absence of Ca, all the following studies were done in Ca-free solutions to reduce the perturbing influence of the pharyngeal nervous system.

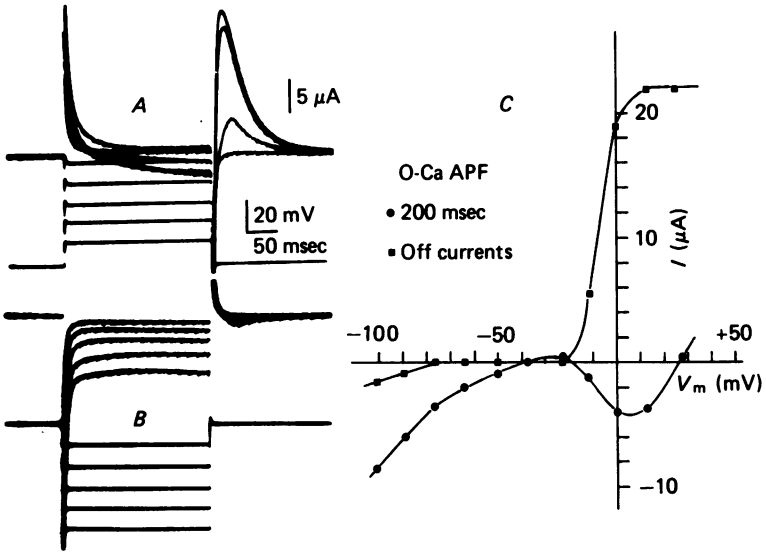

Fig. 4. Single pulse voltage clamps in 0-Ca APF. Upper traces are I_m, lower traces are V_m. All data are from same cell. Holding potential is the resting potential (− 37 mV). *A*, positive voltage pulses. *B*, negative voltage pulses. Calibration same as in *A*. *C*, *I–V* plot. The circles show the current measured at the end (before termination) of the 200 msec pulse as a function of the potential reached by the pulse. The squares show the current 25 msec after the termination of the pulse plotted against the potential of the pulse.

Invagination of external membrane

Del Castillo & Morales (1967*b*) concluded that there is extensive invagination of the external pharyngeal membrane. Not only did electron micrographs show surface membrane invaginations and large (up to 10×10 μm) membrane-bound spaces deep in the muscle, but they recorded with micro-electrodes from extracellular spaces deep within the muscle. By comparing the signal recorded in these deep extracellular spaces with the simultaneous intracellular signal, they concluded that these invaginated membranes are electrically active. We commonly encounter the same deep extracellular spaces while positioning the intracellular electrode. We find additional evidence for these invaginations in both current-clamp and voltage-clamp experiments. When square pulses of inward current are passed through the external

membrane (Fig. 2*B*), the membrane hyperpolarizes with a time constant of 40 msec and reaches a level that indicates that the resistance of all the membrane in the middle compartment is about 10 kΩ. If the area of membrane in the middle compartment is calculated as for a cylinder of the size of the segment of pharynx in that compartment, the membrane specific resistance is found to be 200 Ω cm². Given the 40 msec membrane time constant, this requires a specific capacitance of 200 μF/cm²! This suggests that the area of the invaginations of the external membrane is many times greater than the area of a cylinder of the same dimensions as the segment being studied. When the membrane potential is clamped to small hyperpolarizing voltage pulses, the current shows a large inward capacitance-charging current that decays with a time constant of 5 msec (Figs. 3*B* and 4*B*), even though the monitored membrane potential is stepped to the new level in less than 1 msec. This implies the existence of a large amount of membrane with an appreciable series resistance, as would be expected for the invaginations of the surface membrane.

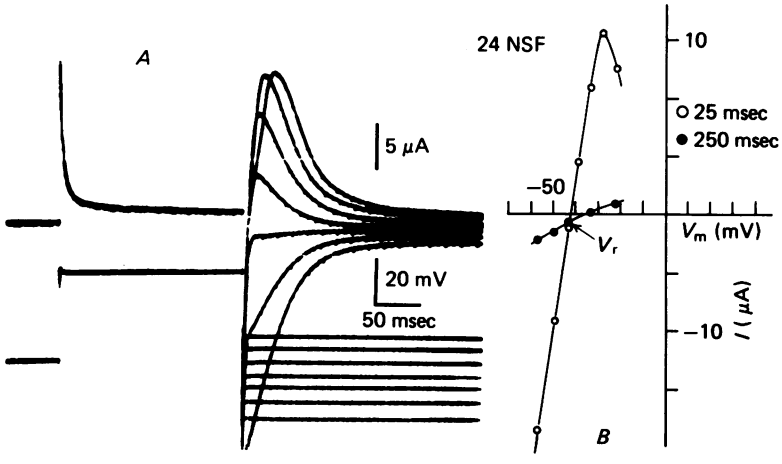

Fig. 5. Reversal of negative spike currents. Cell in 24 NSF. *A*, two-pulse voltage clamp. Upper traces are I_m; lower traces are V_m. Cell is clamped from holding potential (−32 mV) to +5 mV for 200 msec and then back down to different levels. *B*, *I–V* plot. The currents at 25 msec (open circles) and 250 msec (filled circles) after the step down from +5 mV are plotted against the potential of the second pulse. V_r (reversal potential) is −43 mV.

II. *Voltage dependencies of the negative spike current*

The negative spike current observed in voltage-clamp experiments (Fig. 4*A*) is the current that produces the negative action potentials observed in current-clamp experiments (Fig. 2). This identification is supported by three properties common to the two phenomena. (1) Both the negative spike current and the negative-going action potential can only be elicited by negative changes in membrane potential. (2) Both can only be evoked when the membrane potential is depolarized or positive; neither can be evoked when the membrane potential is at the resting level. (3) The reversal potential for the negative spike current is very close to the most negative potential reached by the negative-going action potential. Fig. 5*A* demonstrates a measurement of the reversal potential for the negative spike current. To avoid the

inward capacitance-charging current following the negative step, the negative spike current is measured 25 msec after the step down; this value is plotted against membrane potential in Fig. 5*B*. The reversal potential V_r, the potential at which the negative spike current curve crosses the *I–V* plot for steady-state current (measured at 250 msec), was −43 mV in this particular cell. During current-clamp experiments with this cell, the negative spike was measured to reach the same value within measurement errors. The potential reached by the negative spike and V_r always agreed within errors, as V_r was changed over a 60 mV range by varying $[K^+]_o$.

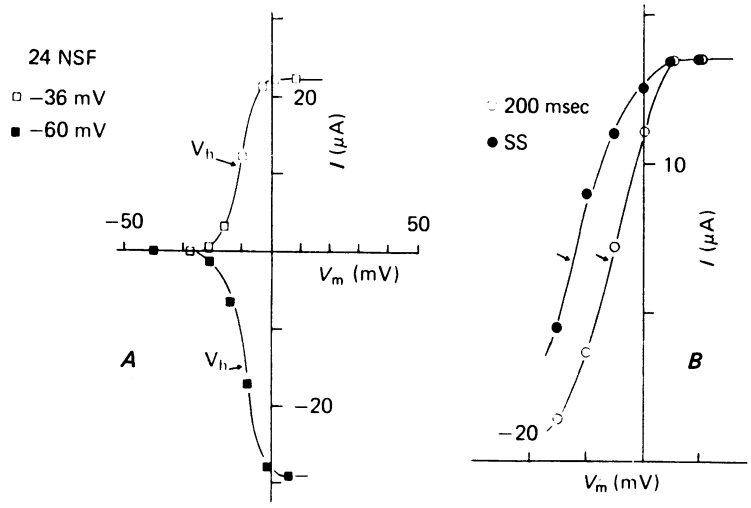

Fig. 6. Inactivation as a function of membrane potential. Cell in 24 NSF. *A*, negative spike current plotted against the conditioning potential at which the membrane is held (for 200 msec) before the negative spike current is turned on. Outward currents (open squares) are obtained when the membrane potential is stepped to −36 mV, and inward currents (filled squares) result when the potential is stepped to −60 mV. V_h (voltage for half removal of inactivation) is −10 mV for steps to −36 mV, and −9 mV for steps to −60 mV. *B*, negative spike current plotted against the conditioning potential at which the membrane was held before turning on the current. The membrane was held at the indicated potential levels for 200 msec (open circles) or for sufficient time to reach a steady state of inactivation (filled circles); membrane potential was stepped to the indicated levels from the resting potential (−34 mV). The negative spike current is triggered by stepping back to the resting potential in both cases. V_h (indicated by arrows) is −6 mV for the 200 msec data and −13 mV for the steady-state data.

Potential dependence of inactivation

The negative spike conductance is completely inactivated when the membrane potential has been at the resting level for times long compared to 30 msec; the membrane potential must be raised to more positive values to remove this inactivation. The absence of a negative spike current when the membrane potential is stepped negatively from the resting potential (Fig. 4*B*) demonstrates that this conductance is inactivated at the resting potential. The appearance of the negative spike when the membrane potential has been held at levels more positive than the resting potential (Fig. 4*A*) can be explained by assuming that the more positive

potentials remove the inactivation of the negative spike conductance. Then, the plot of negative spike current versus the potential at which the membrane was held before the negative spike current was turned on (Fig. 4*C*, squares) becomes a plot of the state of inactivation of the conductance.

If the plot of Fig. 4*C* is a valid measure of the state of inactivation of the conductance before the negative spike current is turned on, it should not be shifted along the voltage axis by a change in the potential to which the membrane is clamped after the positive pulse. Fig. 6*A* shows that this is the case when the negative spike currents are measured as a function of the preceding membrane potential both when stepping back to the resting potential (-36 mV, outward currents) and when stepping back to -60 mV (inward currents). For the cell studied in Fig. 6*A* the membrane has to be held more positive than 0 mV in order to completely remove the inactivation in 200 msec. V_h, the potential at which one half of the inactivation is removed in 200 msec, is about -9 mV for this cell and on average is $-5{\cdot}6 \pm 2{\cdot}0$ ($\pm$ S.D.; $n = 9$). It is seen that some removal of inactivation occurs for potentials as negative as -15 mV.

Time course of inactivation

The removal of inactivation of the negative spike conductances is a slow process at -15 mV, but it becomes faster at more positive potentials. To study the rate of removal of inactivation, we clamped the membrane to more positive potentials for various periods of time and measured the size of the negative spike currents obtained on stepping back to the resting potential; Fig. 7*A* shows the results of such an experiment. After holding the membrane at $+5$ mV for 20 msec, only a small negative spike current is obtained on stepping back to the resting potential. However, the magnitude of the negative spike current increases rapidly with pulse duration and has saturated with pulses longer than 200 msec. In Fig. 7*B* the magnitude of the negative spike current is plotted against the duration of the positive voltage pulse, for conditioning pulses to three different potentials. It is seen that the recovery from inactivation is much more rapid when the membrane is held at a more positive potential. τ^R, the time constant with which inactivation is removed, decreases from values around 300 msec at -15 mV to about 30 msec at $+10$ mV (Fig. 7*C*).

The negative spike currents decay exponentially with time when the membrane is clamped to values more negative than -30 mV (see Fig. 5*A*); in this region the decay time constant, τ^D, is $32{\cdot}0 \pm 5{\cdot}0$ msec and nearly independent of membrane potential. Assuming it is meaningful to compare the time constant measured for current decay with that measured for removal of inactivation, as did Hodgkin & Huxley (1952*c*) when studying the Na current in squid axon, we have plotted τ^D on the same graph as τ^R (Fig. 7*C*). This plot shows that the time constant for the inactivation process has a bell-shaped dependence on membrane potential, reaching a maximum somewhere near -15 mV.

Hodgkin & Huxley also measured the inactivation time constant in a third way, applying depolarizing prepulses; it would seem that we could use a corresponding method to measure the time constant of inactivation between -15 and -30 mV. However, as is demonstrated in Fig. 8*A*, the potential of the invaginated membranes

cannot be controlled between −15 and −30 mV, so the time constant for inactivation cannot be measured in this voltage region.

Since the process of removal of inactivation has not yet reached the steady state by the end of a 200 msec pulse for membrane potentials less than +5 mV, plots of the negative spike current versus the potential of the 200 msec conditioning pulse (such as in Fig. 6*A*) do not show the steady-state inactivation. Fig. 6*B* plots the magnitudes of the negative spike currents measured after 200 msec pulses and after pulses sufficiently long to allow a steady state to be reached. It is seen that the two curves are similar in shape; however, V_h, the potential at which half of the inactivation is removed, is shifted 7 mV more negative for the steady-state curve. We routinely measure the inactivation at 200 msec rather than the steady-state inactivation to avoid depolarizing the cell for long periods of time.

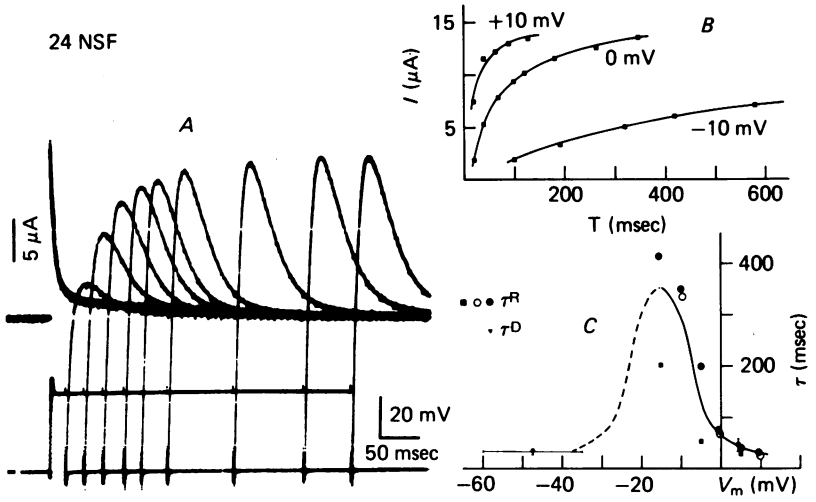

Fig. 7. Rate of removal of inactivation. All cells in 24 NSF. *A*, typical experiment to measure removal of inactivation. Holding potential is resting potential (−32 mV). Cell is clamped to a more positive level (+5 mV) for various lengths of time. Upper traces are I_m; lower traces are V_m. *B*, plot of negative spike currents versus the duration of the positive pulse, for pulses to three different potential levels. *C*, time constant of inactivation as a function of membrane potential. Data points at potentials more positive than −20 mV are τ^R (time constant for removal of inactivation, measured from data as in *B*). This data was taken from three cells (filled squares, open circles and filled circles). The open square with error bars (at +4 mV) indicates the mean and standard deviation of τ^R for eight additional cells. The filled triangle with error bars gives the mean and standard deviation of τ^D (time constant for decay of negative spike current) measured at potentials between −60 and −35 mV, for the same eight cells mentioned above. The curve is drawn by eye; it is drawn with dashes through the region where we have no data.

Voltage dependence of turn-on of negative spike conductance

Once inactivation is removed by holding the membrane at a positive potential, the negative spike current is turned on by stepping the membrane to a more negative potential. This is demonstrated in the experiment of Fig. 8*A*, which shows that the negative spike current becomes recognizable at about −15 mV; when the membrane is stepped to less negative potentials, no outward current flows. Prolonged,

irregularly shaped negative spike currents were almost always obtained when the membrane was stepped to potentials between -15 and -25 mV. These irregularly shaped currents undoubtedly result from a failure of the voltage clamp to control the potential across the deeply invaginated membranes. The failure of the voltage clamp is particularly obvious at -15 to -25 mV, probably because two prolonged voltage-dependent currents, one inward (probably Na) and one outward (negative spike current), are turned on in this region. As the membrane is stepped to levels more negative than -25 mV, the negative spike current rises rapidly (in less than

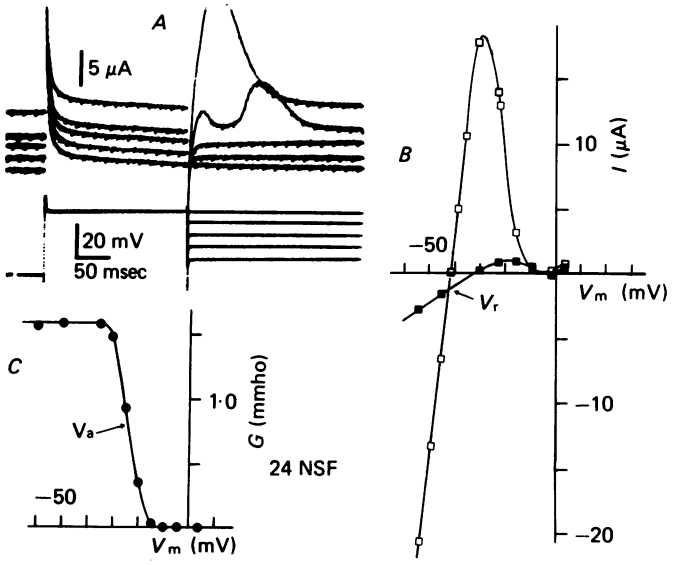

Fig. 8. Voltage dependence of gating mechanism of negative spike current. Cell in 24 NSF. *A*, activation of negative spike current. Cell is stepped from resting potential (-32 mV) to $+4$ mV; after 200 msec the cell is stepped down to different potential levels. Upper traces are I_m (each trace has been shifted vertically from the previous); lower traces are V_m. The lowest current trace corresponds to the voltage trace which remains at $+4$ mV after 200 msec. *B*, *I–V* plot for currents at 25 msec (open squares) and 250 msec (filled squares) after the voltage step down from $+4$ mV. The data for the five most positive voltages has been taken from the traces of *A*. *C*, conductance of the negative spike current as a function of membrane potential. Conductance is calculated as the difference between the two current of *B*, divided by the driving potential, $V_m - V_r$. V_a is the potential at which the conductance is half maximum.

5 msec) and decays exponentially in time, as shown in earlier figures. In spite of the failure of the voltage clamp, a rough measure of the turn on of the negative spike current can be obtained by plotting the currents at 25 msec and 250 msec after the negative step against the potential reached by the negative step (Fig. 8*B*).

A conductance for the negative spike current is calculated by dividing the difference between the two currents plotted in Fig. 8*B* by the driving voltage ($V_m - V_r$); this gives the conductances plotted in Fig. 8*C*. The negative spike conductance starts to turn on at -15 mV and has saturated by -30 mV; the voltage at which the conductance is half turned on, V_a, is -24 mV in this cell. V_a, measured for eight cells in this solution, was $-23{\cdot}7 \pm 1{\cdot}2$ mV. There is considerable variation in the

maximum negative spike conductance measured in different pharyngeal muscles, but typically it is about 1 mmho. Since this is the conductance measured 25 msec after the negative step and the negative spike conductance decays with a time constant of 30 msec, the conductance at the peak of the negative spike current is about 2 mmho. Therefore, the conductance of the membrane is about 20 times larger during the peak of the negative spike than it is at rest (1/10 kΩ) = 0·1 mmho).

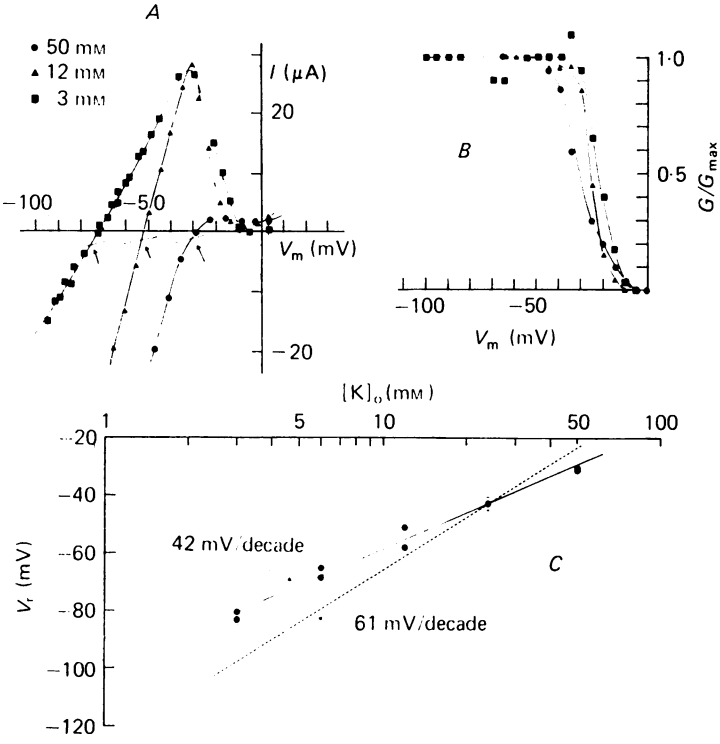

Fig. 9. Dependence of the negative spike current on $[K^+]_o$. Cells in X NSF (see Table 1), where X = 3–50 mM-K^+. *A*, *I–V* plots for three different concentrations of external K^+. Each plot is of the type of Fig. 8*B*. The short line segments, the intersection of which with the curves are indicated by arrows, show the *I–V* curve at 250 msec for that $[K^+]_o$. The data for each $[K^+]_o$ are from a different pharynx, so absolute magnitudes of currents cannot be compared. *B*, normalized conductance versus membrane potential for three different concentrations of K^+. Conductances of the negative spike current have been calculated as in Fig. 8*C*, using the data of part *A* of this Figure; the conductances have been normalized by dividing *G*, the conductance for each $[K^+]_o$, by G_{max}, the maximum conductance obtained at that $[K^+]_o$. *C*, plot of the negative spike reversal potential against the log $[K^+]_o$. Data are taken from eight different cells; the point (with error bars) at 24 mM-K^+ is the mean and standard deviation of the reversal potential measured for all eight cells at 24 mM-K^+. The straight line with a slope of 42 mV/decade is obtained by a least-squares fit. The 61 mV/decade line (dashed) shows the slope expected for a K electrode at 36 °C.

III. *Ionic dependencies of negative spike current*

K *dependence*

The negative spike current was studied in cells bathed with solutions of different concentrations of K^+ (X NSF, X = 3–50 mM, see Table 1). As seen in Fig. 9*A*, the reversal potential for the negative spike current was strongly dependent on $[K^+]_o$.

In Fig. 9*C* the reversal potential V_r has been plotted against the logarithm of $[K^+]_o$. Although the magnitude of the reversal potential depends linearly on log $[K^+]_o$, the slope of 42 mV/decade is less than the 61 mV/decade expected for a K electrode at the temperature of our experiments. This reduced slope could be explained if the prolonged inward current turned on by the positive pulse is not turned off immediately by the step down but persists during the period of the negative spike current. Since the inward current turns on slowly and shows almost no inactivation by the end of a 200 msec pulse (Fig. 4*A*), it seems quite reasonable to suppose that this current would not have turned completely off 25 msec after the step down. Also, a slowly decaying depolarization is frequently observed after the negative spike (Fig. 2*A*), suggesting that the inward current turns off more slowly than does the negative spike current decay. Except for the reversal potential, none of the properties of the negative spike current was changed by altering $[K^+]_o$. When the conductance of the negative spike current was calculated, it was found to always turn on in the same range of potentials, independent of $[K^+]_o$ (Fig. 9*B*). V_h (the potential for half removal of inactivation), τ^D (time constant for current decay) and τ^R (time constant for removal of inactivation) at a given membrane potential were all unchanged by the alterations in $[K^+]_o$.

Actually there was a slight tendency for V_a (the potential at which the conductance is half maximum) to be more negative for higher $[K^+]_o$, i.e. V_a shifts in the opposite direction from the change in E_K. This observed small shift in V_a is in the direction expected when failure of the voltage clamp is considered; with stronger outward currents (obtained in lower $[K^+]_o$) deeply invaginated membranes would have more negative transmembrane potentials than the controlled surface membrane potential. Thus, the negative spike conductance would be measured to turn on more abruptly as a function of surface membrane potential (making V_a more positive) for solutions containing lower concentrations of K^+, even if the gating mechanism for this conductance is independent of $[K^+]_o$. Since this explanation fits well with the small shift observed in V_a, we conclude that the gating mechanism is dependent only on membrane potential (independent of $[K^+]_o$).

Na effect

In experiments intended to examine the possible presence of a Na current during the negative spike current, it was found that V_r does depend on $[Na^+]_o$, but in the opposite sense from that expected. Replacing Na^+ with $Tris^+$ (see Table 1, X Na (Tris) 12 NSF, X = 0–145 mM), V_r becomes more positive and the negative spike conductance decreases as $[Na^+]_o$ is reduced (Fig. 10, squares). In contrast, when Na^+ was replaced with Li^+ there was no significant change in V_r or negative spike conductance. These results could either be interpreted as meaning that Na^+ and Li^+ have a facilitating effect on the negative spike conductance or that $Tris^+$ has an inhibitory effect. To distinguish between these two possibilities, we replaced Na salts with glucose (see Table 1, X Na (glucose) 12 NSF, X = 0–145 mM). In these experiments both V_r and the negative spike conductance varied with $[Na]_o$ exactly as they did when Na^+ was replaced with $Tris^+$ (Fig. 10, circles). Therefore, we favour the conclusion that Na^+ and Li^+ have a facilitating effect on the negative spike conductance. (Ohmori (1978) reported a similar facilitating effect of external egg cell Na^+ and Li^+ on the conductance of the anomalous-rectification channel in tunicate membrane.) This dependence of V_r on $[Na^+]_o$ explains the discrepancy between the slope we measure for V_r against log $[K^+]_o$ and that measured by Del Castillo

& Morales (1967*a*). They found a slope of 65 mV/decade for $[K^+]_o$ between 10 and 50 mM, but they replaced K^+ with Na^+. Thus, the effects of external K^+ and Na^+ were not separated. This facilitating effect of Na^+ on the negative spike current has complicated the picture sufficiently that we remain undecided as to the explanation for the 42 mV/decade slope of the V_r *vs.* $[K^+]_o$ plot.

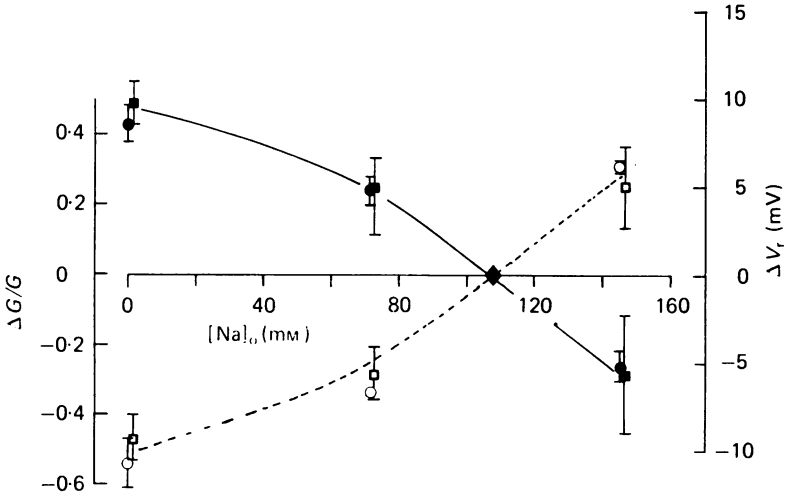

Fig. 10. Effects of external Na^+ on the negative spike current. Data from cells in X Na (Tris) 12 NSF (X = 0–145 mM) are plotted as squares, and data from cells in X Na (glucose) 12 NSF (X = 0–145 mM) are plotted as circles. The open symbols represent the relative change in negative spike conductance $\Delta G/G$ (measured at the reversal potential) and the filled symbols represent the change in reversal potential ΔV_r, when the solution is changed from 107 mM-Na^+ to the indicated $[Na^+]_o$. Each symbol is plotted at the mean for several experiments, and the error bars indicate the range of values from individual experiments.

Blockers

We have tested the effects of a number of the classical K-current blockers on the negative spike current, when applied externally. In Fig. 11 the negative spike conductance with the blocker present is compared to the conductance in the absence of the blocker; chord conductances are calculated between the indicated potentials and V_r. The negative spike current was not significantly reduced by 10 mM-TEA, 10 mM-4-AP, or 1 mM-Ba^{2+}. However, both 10 mM-Rb^+ and 10 mM-Cs^+ show a voltage-dependent blocking. Neither Rb^+ nor Cs^+ cause significant blocking at membrane potentials near the resting potential, but they reduce the negative spike conductance to about half at -100 mV. Rb^+ is also somewhat permeant to the negative spike channel, since V_r is shifted in the positive direction when Rb^+ is added to the external solution; none of the other blockers affects V_r.

DISCUSSION

Comparison with other K currents

The negative spike K current of *Ascaris* pharyngeal muscle is substantially different from the two well known, voltage-dependent K currents. It differs from

the delayed-rectification K current of squid axon (Hodgkin & Huxley, 1952*a*, *b*) in that, while the squid-axon K current is turned on by positive voltage steps and does not inactivate, the negative spike current is turned on by negative voltage steps and inactivates almost completely. In squid axon the K current has a restoring effect on the membrane potential V_m (negative feed-back); it tends to make the membrane potential V_m more negative, opposing the positive shift in V_m that turned it on. The negative spike current has a regenerative effect (positive feed-back) in the pharynx; it also tends to make V_m more negative, which adds to the negative shift

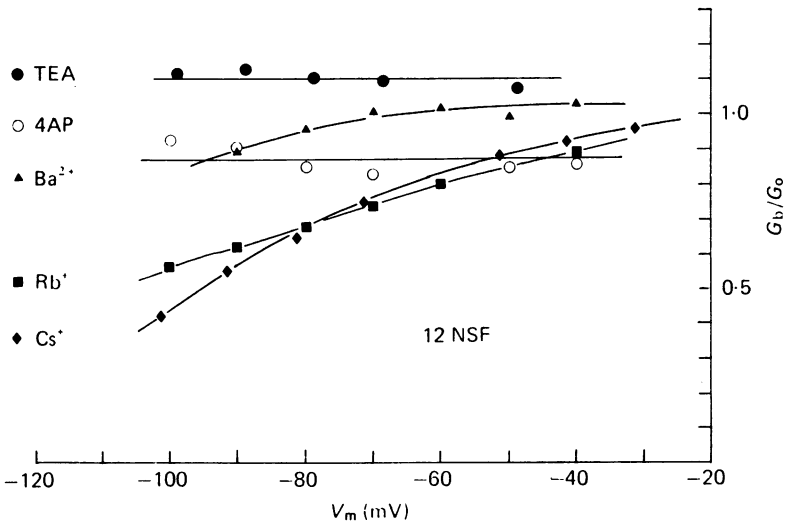

Fig. 11. Effects of various K-current blockers on the negative spike current. G_b/G_o is the ratio of the negative spike conductance in the presence of the blocker to the conductance measured without the blocker. Conductance is calculated as a function of membrane potential in the same manner as explained in Fig. 8*C*. Each blocker is added to 12 NSF; 10 mM-TEA (filled circles), 10 mM-4-AP (open circles), 1 mM-Ba^{2+} (triangles), 10 mM-Rb^+ (squares), 10 mM-Cs^+ (diamonds). Since only two or three cells were tested for each blocker, the systematic errors on the plotted points are fairly large (0·1–0·2).

in V_m that turned it on. The opposite types of feed-back produced by these two currents result from the inverted voltage dependence of their gating mechanisms. The negative spike current differs from the anomalous-rectification K current found in skeletal muscle (Katz, 1949), heart muscle (Hutter & Noble, 1960), and certain egg cells (Takahashi, Miyazaki & Kidokoro, 1971; Hagiwara & Takahashi, 1974), in three ways. (1) The gating mechanism for the anomalous rectification current depends on V_m and $[K^+]_o$ (Almers, 1971; Hagiwara, Miyazaki & Rosenthal, 1976), while the gating mechanism for the negative spike current depends only on V_m. (2) The anomalous-rectification conductance is less than half of its maximum value at $V_m = E_K$ (Almers, 1971; Hagiwara *et al.* 1976); so for a large part of the range of voltages where this conductance is changing, it has a restoring effect on V_m. When the membrane is hyperpolarized from the resting potential (which is near E_K), the K current that is turned on is inward, tending to depolarize the cell. In contrast,

the negative spike current is turned on completely at voltages well above E_K (for normal $[K^+]_o$), so that it has a regenerative effect throughout the range of voltages where this conductance is changing. (3) The anomalous-rectification current does not inactivate as strongly as does the negative spike current. In both frog muscle and tunicate egg the anomalous-rectification current shows almost no true inactivation (see Discussion below) until the membrane is stepped to potentials more negative than -100 mV, although there is 70–80 % inactivation at potentials near -200 mV (Almers, 1972*b*; Ohmori, 1978). The negative spike current appears to almost completely inactivate ($> 95\%$) at all membrane potentials below -30 mV.

The negative spike current is similar to the anomalous-rectification K current in that both currents are turned on by negative potential steps, are not blocked by external TEA, but are blocked in a voltage-dependent manner by Cs^+ (Hagiwara *et al.* 1976). Recently potassium currents have been found in other membranes which are activated by negative steps in potential. Werblin (1975) reported a regenerative hyperpolarization in rods of *Necturus* which was carried by a K current that was turned on by hyperpolarization and showed inactivation. Satow & Kung (1977) studied a regenerative hyperpolarization in *Paramecium*, which was also carried by a K current that was turned on by hyperpolarization. This current differs from the negative spike current in that it does not inactivate and it is blocked by external TEA.

Absence of K accumulation

In frog muscle there is a decline in K conductance during hyperpolarizing pulses due to depletion of K^+ in the transverse tubules (Adrian & Freygang, 1962; Almers, 1972*a*). We have considered and rejected the possibility that the decay of the K current that we observe might be partially due to a similar phenomenon involving the extracellular spaces enclosed by the invaginations of the external membrane. These spaces have a width of about 10 μm, over a hundred times larger than the diameter of the transverse tubules in frog. Since changes in K^+ concentration would be expected to be proportional to the ratio of surface area to volume of the tubular spaces, this effect would be expected to be much more severe in frog muscle than in *Ascaris* pharynx. Assuming the total area of the external membrane to be 5 times the cylindrical surface area of the pharynx and that the invaginations are tubes with a diameter of 10 μm, we calculate that the negative spike current that flows on stepping to -35 mV increases the concentration of K^+ in the tubular volume from 24 to 24·2 mM. This would change E_K from -45 mV to $-44{\cdot}8$ mV, certainly not enough to account for the complete decay of the negative spike current. Since the total area of the membrane and the dimensions of the invaginations are probably greater than we've assumed, it does not seem likely that there is a significant change in the concentration of K^+ in the deep extracellular spaces enclosed by the invaginations of the external membrane. Also, the result that τ^D, the time constant for decay of the negative spike current, does not depend on $[K^+]_o$ argues that the inactivation of the negative spike current is not related to a change in concentration of K^+ in the deep extracellular spaces, since this change in K^+ concentration would probably depend on $[K^+]_o$.

Role of negative spike in pharynx

The pharyngeal membrane appears to have two stable states, the resting potential (about -40 mV) and the plateau of the action potential (around 0 mV), and two regenerative mechanisms for making the transition from one stable state to the other. The voltage-dependent inward current (which is probably Na and Ca, but has not been studied in detail) drives the transition from the resting potential to the plateau, and the negative spike current drives the return from the plateau to the resting potential. Presumably the positive-going transitions are triggered by positive-going post-synaptic potentials (from the pharyngeal nervous system) and the negative-going transitions are triggered by negative-going post-synaptic potentials. (It is possible that both transitions may be triggered by the same transmitter acting on the same receptor, controlling a current with a reversal potential at a level between the two stable states; the pharynx has p.s.p.s which reverse at -10 mV. However, this may well not be the case since the pharynx also has p.s.p.s which reverse at -40 mV.) The two stable states are, of course, not equivalent since the pharynx normally stays at the resting potential and only jumps to the more positive level for brief periods (100–300 msec); however, sometimes (even in APF) the pharynx will stay at the higher level for several minutes.

Analogy between negative spike and Na currents

Except for inverted voltage dependencies, there is a striking analogy between the negative spike current of *Ascaris* and the Na current of squid axon (Hodgkin & Huxley, 1952) and vertebrate skeletal muscle (Campbell & Hille, 1976). (1) Both the Na conductance and the negative spike conductance are controlled by two separate mechanisms, a relatively fast gating mechanism and a slower inactivation mechanism. (2) The gating mechanism of the Na current is opened by depolarization and depends only on membrane potential, independent of $[Na^+]_o$; the gating mechanism of the negative spike current is opened by hyperpolarization and depends only on membrane potential, independent of $[K^+]_o$. (3) Inactivation of both currents is almost complete. (4) The vertebrate skeletal muscle or squid axon membrane has to be held at more negative potentials to remove the inactivation of the Na current; the *Ascaris* pharyngeal muscle membrane has to be held at more positive potentials to remove the inactivation of the negative spike current. (5) The time constant for the inactivation process of Na current is a bell-shaped function of membrane potential, reaching a maximum for those voltages at which the Na conductance is turning on. Although the time constant for the inactivation process of the negative spike current has not been measured between -15 and -30 mV, still it appears to be a bell-shaped function of the voltage, reaching a maximum value in the region of voltages where the negative spike conductance turns on. (6) For both the Na current and the negative spike current the relation between the region of potentials where the conductance is activated (turned on) and the reversal potential for that current is such that regenerative action potentials are produced.

Extending this analogy with the Na conductance, the negative spike conductance can be assumed to have the form, $G_K \propto m^x h$, where m describes the gating process and h the inactivation process. While the pharyngeal cell is resting (see Fig. 12),

the negative spike channels are open ($m = 1$) but inactivated ($h = 0$). When the positive-going action potential first raises the membrane voltage to a positive level, the negative spike channels are rapidly closed ($m \rightarrow 0$) by the change in potential, but there is no immediate change in h. However, during the prolonged depolarization, inactivation is slowly removed ($h \rightarrow 1$); h will eventually reach 1 if the membrane potential is greater than +5 mV. Then when a negative-going post-synaptic potential jumps the membrane negatively, m is increased to a value greater than zero, turning the negative spike current on (h is still one). This current further hyperpolarizes the membrane rapidly increasing m to one. The membrane potential drops to a value near the reversal potential for the negative spike current while the current is strong ($h > 0$). The membrane slowly depolarizes to the resting potential as the negative spike current inactivates ($h \rightarrow 0$).

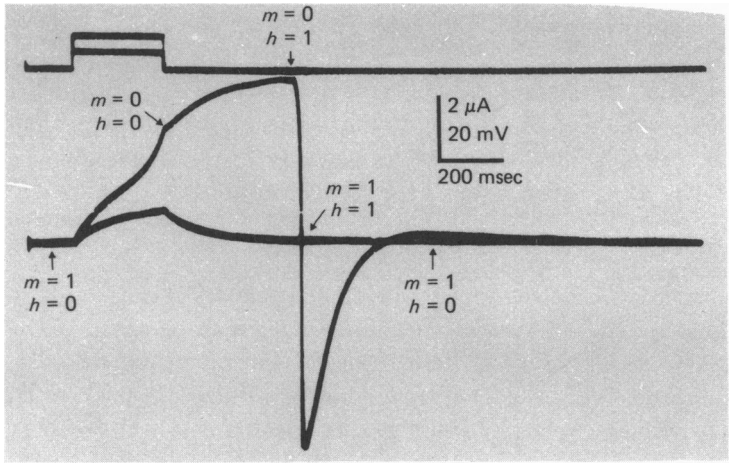

Fig. 12. State of the negative spike conductance during a current-clamped action potential described in terms of Hodgkin & Huxley's m and h parameters. Upper traces are I_m; lower traces are V_m. Cell is in 2 mM-K^+-APF (K^+ replaced with Na^+). The resting potential is −42 mV; the positive action potential reaches +8 mV and the negative action potential reaches −102 mV.

The inversion of the voltage-dependencies between the skeletal muscle Na current and the pharyngeal muscle K current follows from the opposite power phases in the functioning of the two muscles. In both muscles positive membrane potentials elicit contraction. The contraction is the power stroke for skeletal muscle, since this is when the muscle does work on the bones to which it is attached. In order to execute the power stroke quickly, the skeletal muscle has evolved the Na current which produces a positive-going action potential. However, in the pharyngeal muscle the relaxation is the power stroke; contraction of the muscle does no work on the liquid that the pharynx pumps, but only on the internal elastic elements that are stretched by the contraction. In order to pump effectively, the power stroke (relaxation) must be executed quickly. The pharyngeal muscle has achieved this fast relaxation by evolving the K current which produces the negative-going action potential.

We are deeply grateful to Dr Susumu Hagiwara, in whose laboratory this research was conducted, for many valuable suggestions and stimulating discussions. We wish to thank Mr Mac McGlaughlin and Mr Erwin Pachorek for aid in obtaining *Ascaris*. This work was supported by U.S.P.H.S. grant NS09012 to Dr Hagiwara, U.S.P.H.S. fellowship 1F32 NS05479-01 and a Muscular Dystrophy Association Research Fellowship to Dr Byerly, and a fellowship from Conselho Nacional de Desenvolvimento Cientifico e Technologico (CNPq) to Dr Masuda.

REFERENCES

ADRIAN, R. H. & FREYGANG, W. H. (1962). The potassium and chloride conductance of frog muscle membrane. *J. Physiol.* **163**, 61–103.

ALMERS, W. (1971). The potassium permeability of frog muscle membrane. Ph.D. thesis, University of Rochester, Rochester, New York.

ALMERS, W. (1972*a*). Potassium conductance changes in skeletal muscle and the potassium concentration in the transverse tubules. *J. Physiol.* **225**, 33–56.

ALMERS, W. (1972*b*). The decline of potassium permeability during extreme hyperpolarization in frog skeletal muscle. *J. Physiol.* **225**, 57-83.

CAMPBELL, D. T. & HILLE, B. (1976). Kinetics and pharmacological properties of the sodium channel of frog skeletal muscle. *J. gen. Physiol.* **67**, 309-323.

DEL CASTILLO, J., DE MELLO, W. C. & MORALES, T. (1964). Hyperpolarizing action potentials recorded from the esophagus of *Ascaris lumbricoides*. *Nature, Lond.* **203**, 530–531.

DEL CASTILLO, J. & MORALES, T. (1967*a*). The electrical and mechanical activity of the esophageal cell of *Ascaris lumbricoides*. *J. gen. Physiol.* **50**, 603–630.

DEL CASTILLO, J. & MORALES, T. (1967*b*). Extracellular action potentials recorded from the interior of the giant esophageal cell of *Ascaris*. *J. gen. Physiol.* **50**, 631–645.

GOLDSCHMIDT, R. (1904). Der Chromidialapparat Lebhaft Funktionierender Gewebszellen. *Zool. J.* **21**, 41–140.

GOLDSCHMIDT, R. (1910). Das Nervensystem von *Ascaris lumbricoides* und *megalocephala*. *Ein Versuch in den Aufbau eines einfachen Nervensystems einzudrigen*. III. Festschrift zum sechzigsten Geburgstage Richard Hertwigs. chap. 2, pp. 256–354. Jena: Fischer.

HAGIWARA, S. & TAKAHASHI, K. (1974). The anomalous rectification and cation selectivity of the membrane of a starfish egg cell. *J. Membrane Biol.* **18**, 61-80.

HAGIWARA, S., MIYAZAKI, S. & ROSENTHAL, N. P. (1976). Potassium current and the effect of cesium on this current during anomalous rectification of the egg cell membrane of a starfish. *J. gen. Physiol.* **67**, 621-638.

HARRIS, J. E. & CROFTON, H. D. (1957). Structure and function in the nematodes: internal pressure and cuticular structures in *Ascaris*. *J. exp. Biol.* **34**, 116–130.

HODGKIN, A. L. & HUXLEY, A. F. (1952*a*). Currents carried by sodium and potassium ions through the membrane of the giant axon of *Loligo*. *J. Physiol.* **116**, 449–472.

HODGKIN, A. L. & HUXLEY, A. F. (1952*b*). The components of membrane conductance in the giant axon of *Loligo*. *J. Physiol.* **116**, 473–496.

HODGKIN, A. L. & HUXLEY, A. F. (1952*c*). The dual effect of membrane potential on sodium conductance in the giant axon of *Loligo*. *J. Physiol.* **116**, 497–506.

HODGKIN, A. L. & HUXLEY, A. F. (1952*d*). A quantitative description of membrane current and its applications to conduction and excitation in nerve. *J. Physiol.* **117**, 500-544.

HUTTER, O. F. & NOBLE, D. (1960). Rectifying properties of heart muscle. *Nature, Lond.* **188**, 495.

KATZ, B. (1949). Les constantes electriques de la membrane du muscle. *Archs Sci. physiol.* **3**, 285–300.

MAPES, C. J. (1965). Structure and function in the nematode pharynx. *Parasitology* **55**, 269–284.

OHMORI, H. (1978). Inactivation kinetics and steady-state current noise in the anomalous rectifier of tunicate egg cell membrane. *J. Physiol.* **281**, 77–99.

REGER, J. F. (1966). The fine structure of fibrillar components and plasma membrane contacts in esophageal myoepithelium of *Ascaris lumbricoides* (var. *suum*). *J. ultrastruct. Res.* **14**, 602–617.

SATOW, Y. & KUNG, C. (1977). A regenerative hyperpolarization in *Paramecium*. *J. comp. Physiol.* **119**, 99–110.

TAKAHASHI, K., MIYAZAKI, S. & KIDOKORO, Y. (1971). Development of excitability in embryonic muscle cell membranes in certain tunicates. *Science, N.Y.* **171**, 415–418.

WEISBLAT, D. A., BYERLY, L. & RUSSELL, R. L. (1976). Ionic mechanisms of electrical activity in somatic muscle of the nematode *Ascaris lumbricoides*. *J. comp. Physiol.* **111**, 93–113.

WERBLIN, F. S. (1975). Regenerative hyperpolarization in rods. *J. Physiol.* **244**, 53–81.